J. Microbiol. Biotechnol. (2016), 26(1), 160–170
http://dx.doi.org/10.4014/jmb.1505.05060

jmb

Antimicrobial Activity of Bacteriophage Endolysin Produced in *Nicotiana benthamiana* Plants

Natalia Kovalskaya[1]*, Juli Foster-Frey[2], David M. Donovan[2], Gary Bauchan[3], and Rosemarie W. Hammond[1]

[1]*Molecular Plant Pathology Laboratory, U.S. Department of Agriculture, Agricultural Research Service, Beltsville, MD 20705, USA*
[2]*Animal Biosciences and Biotechnology Laboratory, U.S. Department of Agriculture, Agricultural Research Service, Beltsville, MD 20705, USA*
[3]*Electron and Confocal Microscopy Unit, U.S. Department of Agriculture, Agricultural Research Service, Beltsville, MD 20705, USA*

Received: May 19, 2015
Revised: September 16, 2015
Accepted: September 23, 2015

First published online
September 25, 2015

**Corresponding author*
Phone: +1-301-504-5203;
Fax: +1-301-504-5449;
E-mail: natalia.kovalskaya@ars.usda.gov

pISSN 1017-7825, eISSN 1738-8872

The increasing spread of antibiotic-resistant pathogens has raised the interest in alternative antimicrobial treatments. In our study, the functionally active gram-negative bacterium bacteriophage CP933 endolysin was produced in *Nicotiana benthamiana* plants by a combination of transient expression and vacuole targeting strategies, and its antimicrobial activity was investigated. Expression of the *cp933* gene in *E. coli* led to growth inhibition and lysis of the host cells or production of trace amounts of CP933. Cytoplasmic expression of the *cp933* gene in plants using *Potato virus* X-based transient expression vectors (pP2C2S and pGR107) resulted in death of the apical portion of experimental plants. To protect plants against the toxic effects of the CP933 protein, the *cp933* coding region was fused at its N-terminus to an N-terminal signal peptide from the potato proteinase inhibitor I to direct CP933 to the delta-type vacuoles. Plants producing the CP933 fusion protein did not exhibit the severe toxic effects seen with the unfused protein and the level of expression was 0.16 mg/g of plant tissue. Antimicrobial assays revealed that, in contrast to gram-negative bacterium *E. coli* (BL21(DE3)), the gram-positive plant pathogenic bacterium *Clavibacter michiganensis* was more susceptible to the plant-produced CP933, showing 18% growth inhibition. The results of our experiments demonstrate that the combination of transient expression and protein targeting to the delta vacuoles is a promising approach to produce functionally active proteins that exhibit toxicity when expressed in plant cells.

Keywords: Endolysin, vacuolar targeting, potato proteinase inhibitor I, transient expression, *Potato virus* X, *Nicotiana benthamiana*

Introduction

The increasing spread of antibiotic-resistant microorganisms is a growing concern for modern animal production, agriculture, and medicine, and also has a significant negative impact on the US economy [11, 14]. In this regard, phage-encoded endolysins that degrade peptidoglycan (murein) in the cell walls of bacteria, resulting in cell lysis, have acquired significant attention as antimicrobials owing to their high efficiency and mechanism of action [2, 7, 13, 24, 37].

Endolysins are bacteriophage-encoded peptidoglycan hydrolases, which are synthesized in phage-infected cells at the end of the phage lytic cycle [36]. During the process of phage maturation, lysins accumulate in the cytoplasm of infected bacterial cells. Most of the tailed phages possess a holin-endolysin system to achieve the release of their progeny through bacterial lysis. Holin is a small hydrophobic protein produced by double-stranded DNA phages at the end of the lytic cycle and is incorporated into and disrupts the bacterial cytoplasmic membrane, causing the exposure of the cell wall to the peptidoglycan hydrolyses [40, 41]. Alternatively, the lysins containing an N-terminal signal sequence may be exported through the plasma membrane by the host *sec* system [26, 35, 42] or signal-anchor-release system (SAR) [27, 29]. SAR endolysins

that possess a non-cleavable N-terminal type II signal anchor require pinholins (a class of holins) that, at a genetically determined time, cause membrane depolarization and release of the SAR endolysin from the inner membrane into the periplasm, where it refolds and becomes muralytically active [27, 29-31]. Lysins can also interfere with biosynthesis of peptidoglycan, leading to misassembled bacterial cell wall (single-stranded RNA and DNA phages) [12].

Externally applied lysins preferably lyse gram-positive bacteria owing to specific cell organization [13] and therefore could serve as topical antimicrobials or alternatives to antibiotics. The main advantages of lysins versus antibiotics are (i) exogenous lysin application leads to rapid lysis of the bacterial cell wall, avoiding such intracellular resistance mechanisms as efflux pumps, thereby making microbial resistance development rare; and (ii) endolysins possess narrow species specificity without affecting aboriginal (normal) microflora. Numerous studies have shown wide perspectives of lysin usage in human and veterinary medicine as well as in agriculture to control and treat bacterial pathogens, including antibiotic-resistant bacteria [8, 25, 33, 36]. Although the efficiency of lysin application in the treatment and prevention of infectious diseases under laboratory conditions is well established, there is still a need for further investigations in this field before lysin preparations can be approved for human therapy.

In the present study, the antimicrobial properties of the CP933 endolysin, encoded by the cryptic bacteriophage of the gram-negative bacterium *Escherichia coli* O157:H7 str. EDL933 [32], were examined. The *Potato virus* X (PVX)-based vectors pP2C2S and pGD107 [3, 22] were used for transient expression of CP933 in *Nicotiana benthamiana* plants. Although there are distinct advantages of widely used transient-expression systems in plants [6, 23, 34], additional approaches, such as targeting proteins to subcellular compartments [5, 39] or secretory pathways [1, 4, 9, 19], may be required if the target protein is toxic to the host plant and/or for improving recombinant protein accumulation in plants. Murray *et al*. [26] and Jackson *et al*. [15] reported successful targeting of a plant-toxic protein, avidin, to the vacuole in the cells of transgenic tobacco, apple, and sugarcane plants using an N-terminal signal peptide from the potato proteinase inhibitor I (PPI-I) protein. The PPI-I presequence is known to target PPI-I protein constitutively to delta-type vacuoles in potato tubers, and tomato leaves following wound induction [26]. The delta-type vacuoles are distinct from protein storage and lytic vacuoles and harbor pigments and vegetative storage proteins during plant development and in response to environmental triggers [16, 17]. Results of these experiments suggested that the vacuole is the preferable organelle for stable storage of plant transgene proteins that exhibit toxicity to a host plant [26].

In our work, as a result of the toxicity of CP933 to plant cells being revealed during our experiments, the *cp933* coding region was fused at its N-terminus to an N-terminal signal peptide from the PPI-I protein to direct CP933 to delta-type vacuoles. The antimicrobial activity of plant-produced CP933 was evaluated in vitro against *Clavibacter michiganensis* and *E. coli*.

Materials and Methods

Plasmid Constructions

Cloning of the *cp933* gene into the plasmid vector pET21a(+). The complete list of primers used for cloning is shown in Table 1. The genomic sequence encoding the CP933 endolysin originated from the cryptic prophage CP-933P (*E. coli* O157:H7 str. EDL933) and was predicted using BLAST at the National Center for Biotechnology Information (http://www.ncbi.nlm.nih.gov/blast) (GenBank Accession No. NP_287988) [32]. The *cp933* gene was synthesized by Genscript (Piscataway, NJ, USA) and cloned into the pUC57 vector at the NdeI/XhoI restriction sites. The coding region of the *cp933* gene was amplified with the primer pair CP933NdeIF and CP933XhoIR and, after standard cloning procedures, was incorporated into pET21a(+), giving rise to pET21a(+)/*cp933* with the addition of a C-terminal 6×His-tag to facilitate purification of CP933 using Ni-NTA resin.

Cloning of the *ppi-I*, *ppi-I_cp933*, and *ppi-I_gfp* genes into the plasmid vector pET28a+. To direct CP933 to the plant delta vacuole, the coding region of the *cp933* gene was fused at its N-terminus to an N-terminal signal peptide from the PPI-I protein. The overlapping primers NcoIppiF and BamHppiIR were designed based on the sequence of PPI-I [26]. The amplified product was incorporated into the pET28a+ vector at the NcoI/BamHI restriction sites, to produce pET28a+/*ppi-I*. Because of problems with some restriction sites encountered during further cloning procedures, the *ppi-I* gene was amplified from pET28a+/*ppi-I* by PCR using the primer pair NcoIppiF+/EcoRIppiR and incorporated into the pET26b+ plasmid vector, giving rise to pET26b+/*ppi-I*. The resulting plasmid DNAs were digested with BamI/XhoI (plasmid pET28a+/*ppi-I*) and EcoRI/HindIII (plasmid pET26b+/*ppi-I*). The coding regions of the *cp933* and *gfp* genes were amplified from the plasmids pET21a(+)/*cp933* and pGD*smGFP* using primer pairs EcoRICP933F/NotHisCP933R2 and BamHgfpF/XhoIgfpR, respectively, and incorporated into the corresponding plasmids, giving rise to pET26b+/*ppi-I_cp933* and pET28a+/*ppi-I_gfp*. The *ppi-I_cp933* gene was amplified from the plasmid pET26b+/*ppi-I_cp933* using primer pairs NcoIpiF1/HindSHR1 and, after standard cloning procedures, was incorporated into the plasmid vector pET28a+ at the NcoI/HindIII sites, to produce

Table 1. Oligonucleotide primers used for cloning.

Primer	Nucleotide sequence (5′ → 3′)[a]	Restriction sites
CP933NdeIF	ACGTACGTCATATGAACGCAAAAATCAGATACGG	NdeI
CP933XhoIR	ACGTACGTCTCGAGTCTGTCGATTCCCCAGCAC	XhoI
NcoIppiF	TAATCCATGGAGTCAAAGTTTGCTCACATCATTGTTTTCTT**TCTTCTTGCAACTCCCTTTGAAACT**	NcoI
BamHppiIR	TAATGGATCCCTCTGGTCCATCACTTTCTTTTCGTGCCAAGAG**AGTTTCAAAGGGAGTTGCAAGAAGA**	BamHI
NcoIppiF+	TAATCCATGGAGTCAAAGTTTGCTCACATCATTGT	NcoI
EcoRIppiR	TAATGAATTCCTCTGGTCCATCACTTTCTTTTCGT	EcoRI
EcoRIcp933F+	TAACGAATTCGATGAACGCAAAAATCAGATACGGC	EcoRI
NotHisCP933R2	TAATGCGGCCGCTTATCA*GTGATGGTGATGGTGATG*CTCGAGTCTGTCGATT	NotI
BamHgfpF	TAATGGATCCAGTAAAGGAGAAGAACT	BamHI
XhoIgfpR	TAATCTCGAGTCATTATTTGTATAGTTCATCCA	XhoI
NcoIpiF1	TAATCCATGGAGTCAAAGT	NcoI
HindSHR1	TAATAAGCTTTTATCA*GTGAT*	HindIII
CP933F	TAACGATATCAACAATGGCTAACGCAAAAATCAGATA	EcoRV
EcoRVStopHisR	TAACGATATCTTATCA*GTGATGGTGATGGTGATG*	EcoRV
EcoRVppiF	TAACGATATCAACAATGGCTGAGTCAAAGTTTGCTCA	EcoRV
EcoRVgfpF	TAACGATATCAACAATGGCTAGTAAAGGAGAAGAACT	EcoRV
EcoRVgfpR	TAACGATATCTCATTATTTGTATAGTTCATCCATGCCA	EcoRV
EcoRVppiF	TAACGATATCAACAATGGCTGAGTCAAAGTTTGCTCA	EcoRV
MluKozCP933F	TAACACGCGTCCACCATGGCAAACGCAAAAATCAGATAC	MluI
NotHisCP933R2	TAATGCGGCCGCTTATCA*GTGATGGTGATGGTGATG*CTCGAGTCTGTCGATT	NotI
MluKozppiIF	TAACACGCGTCCACCATGGCAGAGTCAAAGTTTGCT	MluI

[a]Restriction sites are underlined; nucleotides in italics encode the 6×His-tag; overlapping regions are shown in bold.

pET28a+/*ppi-I_cp933*.

Cloning of the *cp933*, *ppi-I_cp933*, *gfp*, and *ppi-I_gfp* genes into the PVX-based vector pP2C2S. The coding regions of the *cp933*, *ppi-I_cp933*, *gfp*, and *ppi-I_gfp* genes were amplified from the plasmids pET21a(+)/*cp933*, pET28a+/*ppi-I_cp933*, pGD*smGFP*, and pET28a+/*ppi-I_gfp*, using primer pairs CP933F/EcoRVStopHisR, EcoRVppiF/EcoRVStopHisR, EcoRVgfpF/EcoRVgfpR, and EcoRVppiF/EcoRVgfpR, respectively. The PCR products were incorporated into the pP2C2S vector at the EcoRV site, giving rise to pP2C2S/*cp933*, pP2C2S/*ppi-I_cp933*, pP2C2S/*gfp*, and pP2C2S/*ppi-I_gfp*, respectively.

Cloning of the *cp933* and *ppi-I_cp933* genes into the binary PVX-based vector pGR107. The multiple cloning site (MCS) of the vector pGR107 (a gift of Dr. David Baulcombe, Sainsbury Centre, UK [22]) was modified to incorporate additional restriction sites (not shown). The available restriction sites in the expanded MCS included MluI, CalI, SmalI, SalI, and NotI. The *cp933* and *ppi-I_cp933* genes were amplified from pET21a(+)/*cp933* and pET28a+/*ppi-I_cp933* using primer pairs MluKozCP933F/NotHisCP933R2 and MluKozppiIF/NotHisCP933R2, respectively, and were cloned into plasmid vector pGR107 at the MluI/NotI sites, giving rise to pGR107/*cp933* and pGR107/*ppi-I_cp933*.

All constructs were verified by direct DNA sequencing.

Preparation and Delivery of Infectious Transcripts

Capped transcripts from SpeI-linearized pP2C2S/*cp933*, pP2C2S/*ppi-I_cp933*, pP2C2S/*gfp*, and pP2C2S/*ppi-I_gfp* plasmids were generated with the mMessage mMachine T7 kit (Ambion, Austin, TX, USA), diluted twice with 20 mM sodium phosphate buffer (pH 7.0), and rubbed onto three top carborundum-dusted leaves of *N. benthamiana* plants. Inoculated plants were grown in a greenhouse at 27 ± 2°C under 18 h light and 6 h dark photoperiods until protein extraction was performed.

Transformation of *Agrobacterium tumefaciens* and Agroinfiltration

Introduction of pGR107/*cp933* and pGR107/*ppi-I_cp933* into *A. tumefaciens* and agroinfiltration of *N. benthamiana* plants were performed using procedures previously described [21].

RT-PCR for Detection of *cp933* and *ppi-I_cp933* Genes in Plants

Total cellular RNA was extracted by TRI Reagent (Molecular Research Center, Inc., Cincinnati, OH, USA) from systemically infected *N. benthamiana* leaves 1 week after inoculation with PVX RNA transcripts or agroinfiltration. RT-PCR analysis was carried

out using the Titan One Tube RT-PCR System (Roche Molecular Biochemicals, Chicago, IL, USA) as described in the manufacturer's instruction and using the primer pairs CP933F/EcoRVStopHisR, EcoRVppiF/EcoRVStopHisR, MluKozCP933F/NotHisCP933R2, and MluKozppiIF/NotHisCP933R2 (0.4 pmol final concentration) for pP2C2S/*cp933*, pP2C2S/*ppi-I_cp933*, pGR107/*cp933*, and pGR107/*ppi-I_cp933*, respectively. For RT-PCR, 35 cycles were conducted in a GeneAmp System 9700 (Applied Biosystems, Foster City, CA, USA) with AMV reverse transcriptase for the first-strand cDNA synthesis and the Expand High Fidelity enzyme blend (Roche) consisting of Taq DNA polymerase and Tgo DNA polymerase for amplification of cDNA by PCR. The PCR fragments were fractionated on a 1.0% agarose gel.

Protein Extraction and Characterization

Protein production in bacteria. To produce CP933 protein in bacteria, the construct pET21a(+)/*cp933* was introduced into *E. coli* strains BL21(DE3) (Stratagene, La Jolla, CA, USA), C43(DE3) pLysS, C43(DE3), C41(DE3) pLysS, and C41(DE3) (Lucigen, Middleton, WI, USA) according to the manufacturer's instructions. Protein induction, extraction, inclusion body (IB) purification, solubilization, and refolding were performed as previously described [20].

Protein extraction from *N. benthamiana* and purification. Protein extraction from plant tissues was performed using 1× PBS buffer (Bio-Rad, Hercules, CA, USA) or 10 mM Tris-HCl, pH 8.0, containing 8 M urea. Both buffers were supplemented with a 1:100 dilution of a plant protease inhibitor cocktail (Sigma Chemical Co., St. Louis, MO, USA). After two rounds of centrifugation (at 4,000 ×*g* for 20 min and at 10,000 ×*g* for 10 min) for extracts in 1× PBS buffer and six rounds of centrifugation (one round at 4,000 ×*g* for 20 min and five rounds at 10,000 ×*g* for 10 min) for extracts in 8 M urea buffer, the protein samples were analyzed by western blot assay or purified using Ni-NTA resin after filtration through 0.22 µm low protein binding membrane filter (Millipore Corporation, Bedford, MA, USA). For purification, filtered protein samples obtained with 1× PBS buffer were applied to a column with 1 ml of Ni-NTA resin pre-washed with 1× PBS containing 10 mM imidazole and incubated for 1 h at 4°C, with rotation. Columns were washed with 3 column volumes of 1× PBS containing 20 mM imidazole and bound protein was eluted twice with 500 µl and 300 µl of 1× PBS containing 500 mM imidazole. Eluted fractions were combined and dialyzed against 1× PBS overnight at 4°C. In the procedure where proteins were extracted using 8 M urea buffer, protein samples were applied to a column with 1 ml of Ni-NTA resin pre-washed with 7 M urea buffer, pH 8.0, and incubated for 1 h at 4°C, with rotation. Columns were washed with 3 column volumes of 8 M urea buffer, pH 6.3, and bound protein was eluted twice with 500 µl and 300 µl of 8 M urea buffer, pH 4.5. The eluted fractions were combined and dialyzed against 20 mM Tris-HCl, pH 8.0, overnight at 4°C. The resulting protein samples were analyzed by western blotting and used for antibacterial assays after filtration through a 0.22 µm low protein binding membrane filter (Millipore Corporation). To determine the concentration of purified protein samples, measurement of absorbance at 280 nm was performed (Thermo Scientific NanoDrop ND-8000 8-Sample Spectrophotometer).

Gel electrophoretic and western blot analyses of proteins. Aliquots of the CP933 protein produced in bacteria or plants were electrophorized on a Novex Tris-Glycine Gradient Gel (10% to 20%; Invitrogen) under denaturing conditions as described in the manufacturer's instructions. The protein was visualized by staining with SimplyBlue SafeStain (Invitrogen). Alternatively, proteins were transferred to a nitrocellulose membrane (following manufacturer's instructions; Invitrogen) that was subsequently incubated with 1:1,000 dilution of Anti-His HRP Conjugate solution (Penta His HRP Conjugate Kit; 5 Prime Inc., Gaithersburg, MD, USA) according to the manufacturer's instruction, followed by membrane development using the TMB Membrane Peroxidase Substrate System (KPL, Gaithersburg, MD, USA).

Confocal laser scanning microscopy (CLSM). Transverse sections (approx. 0.2 mm) and pieces of fresh leaves of *N. benthamiana* were excised and placed in cover glass-bottom Petri dishes (MatTeck Corp., Ashland, MA, USA) for observation. A Zeiss LSM710 CLSM system (Thornwood, NY, USA) was used to obtain images. The images were observed using a Zeiss Axio Observer inverted microscope with 40× 1.3 NA Plan-Apochromat water immersion objectives. A 488 nm argon laser with a pin hole of 30 µm passing through a MBS 488 beam splitter filter with limits set between 495 and 535 nm was used. The Zeiss Zen 2012 (Thornwood, NY, USA) 64 bit software was used to obtain images. Forty to seventy 30 µm per frame z-stack images were obtained to produce 3D renderings, which were used to develop the 2D maximum intensity projections for publication.

Microorganisms

Clavibacter michiganensis subsp. *sepedonicus* (hereinafter referred to as *C. michiganensis*), a gram-positive bacterium causing potato ring rot disease, was cultivated on nutrient-broth yeast extract agar (NBY) [21] at 25ºC. For antibacterial assays, NBY broth was inoculated with the colonies from the plate and incubated at 25ºC with shaking at 250 rpm for 5 days.

E. coli BL21(DE3) (Stratagene), a gram-negative bacterium, was transformed with pET26b+ plasmid for growth on YT medium supplied with kanamycin. For antibacterial assays, the colonies from the plate were transferred into YT broth containing kanamycin and incubated overnight at 37ºC with shaking at 250 rpm.

Antibacterial Assays

The antibacterial activity of the plant-produced and purified CP933 protein was examined against *C. michiganensis* and *E. coli* as previously described [20], using a final protein concentration of 54 µg/ml in 500 µl of total reaction volume. The bacterial concentration before experiment was 5.6×10^4 colony-forming units (CFU)/ml for *C. michiganensis* and 3.6×10^5 CFU/ml for *E. coli*. The reaction mixtures were incubated at 25ºC and 37ºC

with shaking at 250 rpm for 5 days and 17 h for *C. michiganensis* and *E. coli*, respectively. Following incubation, 100 µl aliquots of protein-treated bacterial cultures were serially diluted in sterile water (from 10^{-2} to 10^{-6}) and 25 µl of diluted bacterial suspensions was plated onto the appropriate solid medium. The plates were incubated at 25°C and 37°C for 5 days and 17 h for *C. michiganensis* and *E. coli*, respectively, and the bacterial growth was examined by counting CFU. Each experiment has at least three repetitions. The data are expressed as the mean ± the standard error of the mean. Statistical significance of obtained data was analyzed by calculating the *p*-value (http://www.socscistatistics.com).

Results

In order to examine the antimicrobial properties of CP933, we attempted to produce the protein in a prokaryotic expression system. The *cp933* gene was subcloned into the pET21a(+) plasmid vector under the transcriptional control of the bacteriophage T7 promoter (Fig. 1A) and introduced into *E. coli* strains BL21(DE3), C43(DE3) pLysS, C43(DE3), C41(DE3) pLysS, and C41(DE3), as described in Materials and Methods. Expression of the *cp933* gene in bacterial cells led to growth inhibition and lysis of the host cells (strains BL21(DE3), C43(DE3) pLysS, and C41(DE3) pLysS) or production of trace amounts of the CP933 (strains C43(DE3) and C41(DE3)). Analysis of both total and soluble fractions of CP933 protein showed that it was localized in the total fraction containing insoluble inclusion bodies (Fig. 2A). Expression of *cp933* in *E. coli* was confirmed by western blot analysis (Fig. 2B). The attempt to purify the bacterially produced protein with Ni-NTA resin failed owing to the extremely low yield of protein.

To overcome the expression problems encountered in *E. coli*, we explored the possibility of producing the CP933 protein in *N. benthamiana* plant cells. The *cp933* gene containing a 6× His-tag at its C-terminus was engineered into the PVX-based transient expression vector pP2C2S [3] and binary PVX-based vector pGR107 [22], under the transcriptional control of the bacteriophage T7 and

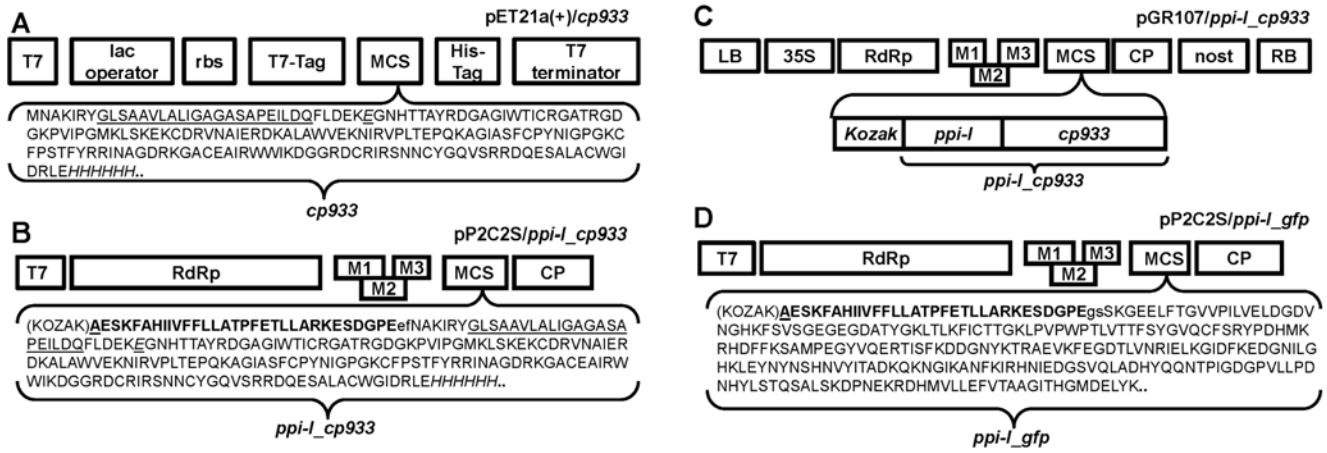

Fig. 1. Schematic representation of vector constructions carrying *cp933* and fusion genes *ppi-I_cp933* and *ppi-I_gfp*.
The cloning/expression region of pET21a(+)/*cp933* vector indicating the insertion of the *cp933* gene (**A**). pET21a(+) carries an N-terminal T7-Tag sequence, optional C-terminal His-Tag sequence, ribosomal binding site (rbs) sequence. CP933 is a positively charged protein, rich in hydrophobic amino acids. The amino acid sequence of CP933 has a total of 187 amino acids (aa), including 22 aa of the transmembrane domain (underlined); 1 catalytic residue (italics with underlining), 6 histidine residues (italics), and 2 stop codons (dots). Genome organization of PVX-based vectors carrying fusion gene *ppi-I_cp933*: pP2C2S/*ppi-I_cp933* (**B**), pGR107/ *ppi-I_cp933* (**C**), and pP2C2S/*ppi-I_gfp* (**D**). Transcription of fusion constructs was driven by the duplicated coat protein subgenomic promoter. Features shown are T7 bacteriophage (T7) and *Cauliflower mosaic virus* 35S (35S) promoters; viral RNA-dependent RNA polymerase gene (RdRp); "triple gene block" encoding three specific movement proteins of PVX: M1, M2, M3; multiple cloning site (MCS); coat protein (CP); nopaline synthase transcriptional terminator (*nos*t); and T-DNA left and right borders (LB, RB). The amino acid sequence of PPI-I_CP933 has a total of 220 aa: 31 aa of PPI-I sequence (in bold), containing the cleavage site between 23 and 24 aa, 178 aa of CP933 sequence (including 22 aa of the transmembrane domain (underlined) and 1 catalytic residue (italics with underlining)), 1 additional alanine residue after the start codon (bold underlined), 6 histidine residues (italics), 2 aa corresponding to the restriction site between *ppi-I* and *cp933* genes (lowercase), and 2 stop codons (dots). The amino acid sequence of PPI-I_GFP has a total of 272 aa, including 31 aa of PPI-I (in bold), 236 aa of GFP sequence, 1 additional alanine residue after the start codon (bold underlined), 2 aa corresponding to the restriction site between *ppi-I* and *gfp* genes (lowercase), and 2 stop codons (dots). The start codon (ATG) in all PVX-based constructs was placed in the surrounding plant translational consensus sequence (Kozak).

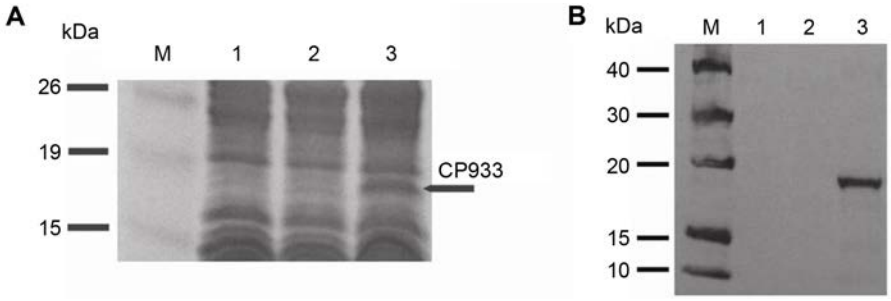

Fig. 2. SDS-PAGE and Western blot analysis of *E. coli*-produced CP933.
SDS-PAGE (**A**) and Western blot (**B**) analysis using 1:1,000 dilution of Anti-His HRP Conjugate solution (Penta His HRP Conjugate Kit, 5 Prime Inc., Gaithersburg, MD, USA) followed by membrane development by TMB Membrane Peroxidase Substrate System (KPL, Gaithersburg, MD, USA). Lanes: 1, uninduced control (without addition of IPTG); 2 and 3, soluble and total fractions, respectively, of CP933 produced in *E. coli* strain C41(DE3). kDa = BenchMark Pre-Stained Protein Ladder (Novex, Life Technologies, CA, USA) for SDS-PAGE and BenchMark His-tagged Protein Standard (Novex, Life Technologies, CA, USA) for the western blot. Predicted MW CP933 = 20.7 kDa.

Cauliflower mosaic virus 35S promoters, respectively, with the expectation that the CP933 protein would be expressed in the cytoplasm of plant cells. Expression of the *cp933* gene from both of these vectors resulted in growth inhibition and death of the apical region of experimental plants after 10 dpi (Fig. 3C). Western blot analysis did not detect the presence of CP933 in plants producing cytoplasmic CP933. Moreover, the collection of plant samples was complicated by the low quality of plant material due to the negative impact of CP933 on plants. The lower, initially uninfected leaves remained uninfected during the period of experiment, so they could not be used for protein extraction. To protect plants against the detrimental impact of CP933, the *cp933* gene was fused at its N-terminus to an N-terminal signal peptide from PPI-I (Figs. 1B and 1C) to direct CP933 to delta-type vacuoles. To verify the ability of the PPI-I signal peptide to target a protein of interest to a vacuole, we designed a construct containing the *gfp* reporter gene (pP2C2S/*ppi-I_gfp*) (Fig. 1D), introduced it into the *N. benthamiana* plants, and examined GFP localization in the cells of systemically infected leaves on the 10th dpi. Confocal microscopy showed expected autofluorescence in *N. benthamiana* cells (Figs. 4A and 4B) of the "control-mock" (plants treated with 20 mM sodium phosphate buffer) and "empty-pP2C2S" (plants infected with empty pP2C2S vector) experimental groups, and confirmed the vacuolar localization of GFP in infected *N. benthamiana* leaf mesophyll cells (Fig. 4D) compared with its primary localization in the nucleus and cytoplasm in the construct lacking the PPI-I signal peptide (Fig. 4C).

We next examined the expression of the *ppi-I_cp933* gene in *N. benthamiana* as described in Materials and Methods.

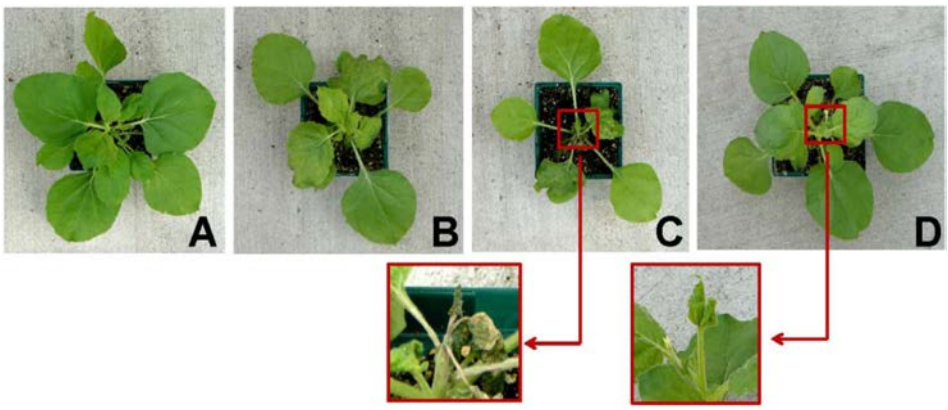

Fig. 3. Effect of CP933 on growth of *N. benthamiana* plants.
Representative *N. benthamiana* plants of the following experimental groups (10 dpi): "control-mock" (**A**), "empty-pP2C2S" (**B**), "pP2C2S/*cp933*" (cytoplasmic gene expression) (**C**), and "pP2C2S/*ppi-I_cp933*" (vacuolar targeting) (**D**).

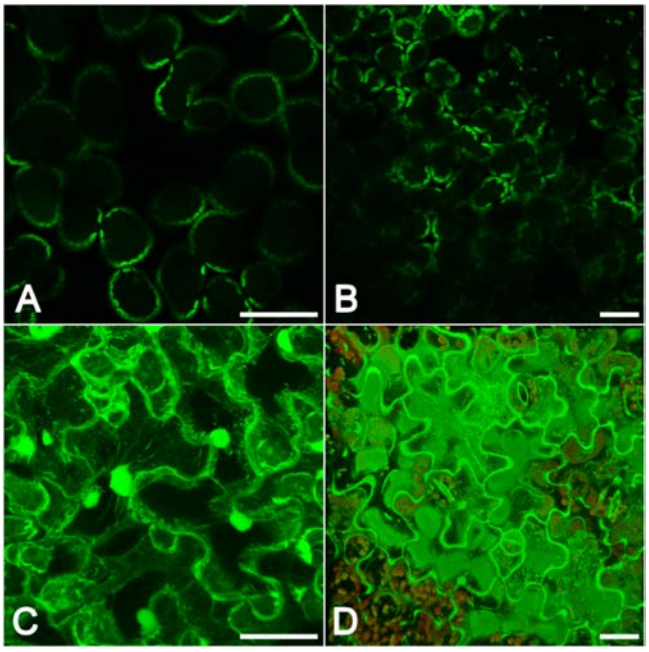

Fig. 4. GFP localization in systemically infected *N. benthamiana* leaves (10 dpi).
Confocal laser scanning microscopy showed autofluorescence in *N. benthamiana* cells of "control-mock" (**A**) and "empty-pP2C2S" (**B**) experimental groups, GFP localization in the cytoplasm and nucleus ("pP2C2S/*gfp*") (**C**), and vacuolar localization of GFP in infected *N. benthamiana* leaf mesophyll cells (**D**) ("pP2C2S/*ppi-I_gfp*"). Chloroplast autofluorescence is shown in red. Scale bars: 50 μm.

Plants producing the vacuolar-targeted PPI-I_CP933 fusion did not exhibit the severe phenotypic symptoms (Fig. 3D) observed with cytoplasmic expression of *cp933* (Fig. 3C). The fact that plants producing the fusion protein PPI-I_CP933 remained phenotypically normal indicates that targeting was successful.

The stability of the *cp933* and *ppi-I_cp933* genes within

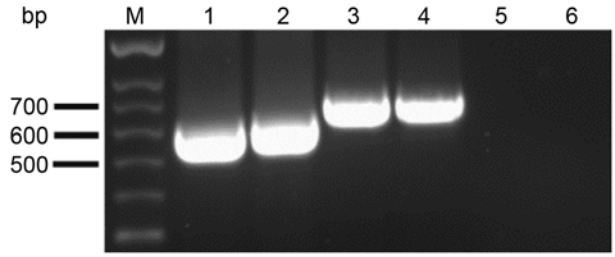

Fig. 5. RT-PCR analysis of total cellular RNA isolated from the systemically infected *N. benthamiana* leaves (8 dpi).
Lanes: 1 and 2, "pP2C2S/*cp933*"; 3 and 4, "pP2C2S/*ppi-I_cp933*"; 5, "empty-pP2C2S"; 6, "control-mock" (healthy plant); "M", DNA marker: Hyper Ladder II (Bioline).

the PVX-based vector in *N. benthamiana* plants was confirmed by RT-PCR assays performed on RNA samples isolated from systemically infected leaves at 8 dpi (Fig. 5).

The plant-produced PPI-I_CP933 fusion protein was extracted and purified with Ni-NTA resin at 7–10 dpi. Western blot analysis using His-tag specific antibodies confirmed CP933 protein production in systemically infected *N. benthamiana* leaves (Fig. 6). A difference in migration of the CP933 protein on the gel was dependent on the buffer used for protein extraction from plant tissues. The molecular weight of the detected protein was consistent with the predicted molecular mass of the fusion PPI-I_CP933 after cleavage (21.6 kDa) (Fig. 6A) when the 1× PBS extraction method was used. However, when 8 M urea buffer, pH 8.0, was employed for protein extraction and purification, the estimated molecular weight of the CP933 product was twice that of the predicted molecular mass (Fig. 6B). The level of production of fusion CP933 in plants was 0.16 mg per gram of plant tissue.

To test the antimicrobial activity of the plant-produced endolysin, we performed growth inhibition assays using

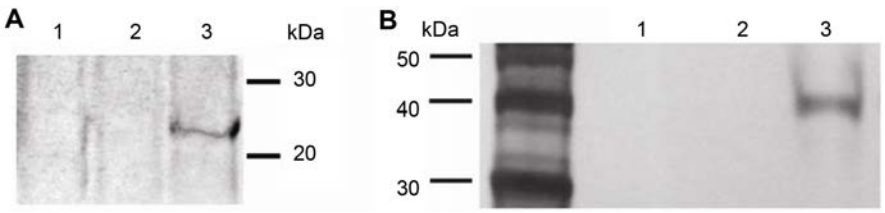

Fig. 6. Western blot analysis of CP933 expressed in *N. benthamiana*.
Western blot analysis of total protein fraction extracted from systemically infected *N. benthamiana* leaves with 1× PBS (**A**) and 8 M urea in 10 mM Tris-HCl, pH 8.0 (**B**) (7 dpi). The membrane was incubated with 1:1,000 dilution of Anti-His HRP Conjugate solution (Penta His HRP Conjugate Kit; 5 Prime Inc., Gaithersburg, MD, USA) followed by membrane development by TMB Membrane Peroxidase Substrate System (KPL, Gaithersburg, MD, USA). Lanes: 1, "control-mock" (healthy plant); 2, "empty-pP2C2S"; and 3, "pP2C2S/*ppi-I_cp933*" (vacuolar targeting). Predicted MW of PPI-I_CP933 after cleavage is 21.6 kDa.

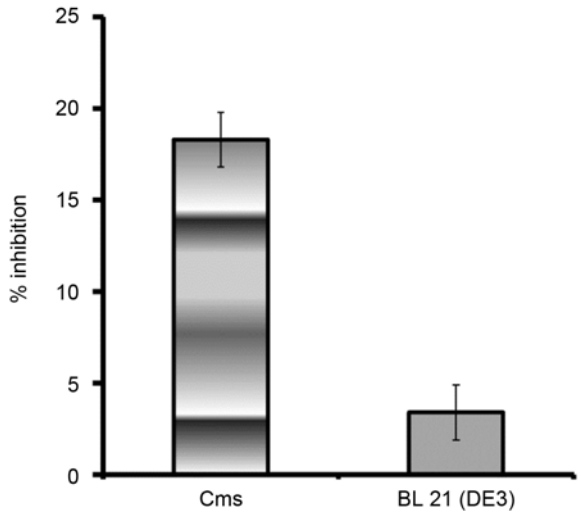

Fig. 7. Antimicrobial activity of plant-produced CP933 protein (54 μg/ml) against *C. michiganensis* (Cms) and *E. coli* BL21(DE3). "% inhibition" on the Y-axis refers to CFU for the bacterium: *C. michiganensis* (18.3 ± 1.5) and *E. coli* (3.4 ± 2.0). Inhibition of *C. michiganensis* was statistically significant ($p < 0.05$).

the PPI-I_CP933 protein, as described in Materials and Methods. The experiments demonstrated that, in contrast to *E. coli*, *C. michiganensis* was more susceptible to treatment with CP933, showing statistically significant 18% growth inhibition ($p < 0.05$ (0.006)) (Fig. 7).

Discussion

In this study, the CP933 endolysin encoded by a cryptic prophage CP-933P (*Escherichia coli* O157:H7 str. EDL933) was produced in *N. benthamiana* plants using a PVX-based transient expression vector, and its antimicrobial activity was evaluated in vitro against the gram-positive bacterium *C. michiganensis* and the gram-negative bacterium *E. coli* BL21(DE3).

Prior to producing CP933 in plants, we attempted to express the *cp933* gene in a prokaryotic expression system. Several strains of *E. coli* were chosen (BL21(DE3), C43(DE3) pLysS, C43(DE3), C41(DE3) pLysS, and C41(DE3)), but only two that were specially designed for toxic protein production were able to produce CP933 (strains C43(DE3) and C41(DE3)), although at unsatisfactory levels. Strains C43(DE3) and C41(DE3) were derived from C41(DE3) and BL21(DE3), respectively, and are suitable for production of protein from the genes cloned into expression vectors under the control of the T7 promoter (http://www.lucigen.com).

The mode of action of CP933 is not completely known. Analysis of the CP933 amino acid sequence revealed that it is a positively charged protein, rich in hydrophobic amino acids. Bioinformatic comparison of the predicted CP933 amino acid sequence with the complete genome sequences of all endolysins found in double-stranded DNA and RNA phages [27] revealed that CP933 contains an N-terminal transmembrane domain with a catalytic residue (Fig. 1A), suggesting that CP933 belongs to the SAR family of endolysins. Moreover, according to the literature, SAR endolysins were encoded only by phages of gram-negative bacteria, mostly from the Enterobacteriaceae family, with few exceptions [27]. In the SAR system, the non-cleavable N-terminal transmembrane domain, being a part of the mature endolysin, stays embedded in the plasma membrane in an enzymatically inactive form during the latent period until membrane depolarization caused by pinholin activity [27, 29, 30, 31]. However, the robust lytic activity of recombinant CP933 in *E. coli*, when pinholin is not available, is most likely explained by the impact of positively charged CP933 endolysin, primarily, on negatively charged bacterial membrane, leading to membrane disruption, followed by enzymatic degradation of the cell wall peptidoglycan in bacteria. This hypothesis leads us to speculate that CP933 may also affect the plant cell wall or membrane or both when expressed in the cytoplasm, leading to collapse of rapidly growing plant tissues. It was reported that some lysins, especially those originating from phages of gram-negative bacteria, are capable of affecting bacterial cells in an enzymatic-independent way. It was found that some endolysins contained a sequence in the C-terminus similar to a sequence of cationic antimicrobial peptides [10, 28]. Düring *et al*. [10] showed that T4 lysozyme, derived from the phage of a gram-negative bacterium, contained in its sequence at least one positively charged α-helix domain that consisted of basic amino acid residues able to interact with the negatively charged bacterial membrane. It has also been shown that synthetic peptides with an amino acid sequence corresponding to the sequence of this helix possessed strong bactericidal and not enzymatic activity.

Furthermore, the impact of plant viral vector itself on plant tissues cannot be excluded. In our previous studies, we observed the synergistic effect of co-infection by the empty-PVX-based vector and the phytopathogenic fungus *Colletotrichum coccoides* that led to plant collapse [21]. However, in the present study, the absence of the toxic effect in plants expressing vacuolar-targeted CP933 using PVX-based vectors (pP2C2S/*ppi-I_cp933* or pGR107/*ppi-I_cp933*) indicates that the vectors themselves do not play a crucial role in the severe symptom development (growth

inhibition and death of the plant apical region) that was observed in the case of cytoplasmic protein expression (pP2C2S/*cp933* or pGR107/*cp933*). Therefore, we concluded that the phenotypic changes in plants producing CP933 (pP2C2S/*cp933* or pGR107/*cp933*) in the cytoplasm were primarily a result of CP933 activity.

To protect plants against the detrimental impact of CP933, the *cp933* gene containing a 6×His-tag at its C-terminus was fused at its N-terminus to the PPI-I signal peptide to direct CP933 to delta-type vacuoles. The successful expression of plant-toxic proteins in transgenic tobacco leaves and sugarcane through the use of vacuolar targeting was shown for the biotin-binding proteins avidin and streptavidin [15, 26]. Targeting to the delta vacuoles resulted in the high yields of avidin for both plants and streptavidin for tobacco plants, although in sugarcane a biotin-deficient phenotype was observed [15]. Tobacco plants appeared phenotypically indistinguishable from non-transgenic plants [26]. In our attempt to express the endolysin gene in *N. benthamiana*, a combination of transient expression and vacuole targeting strategies were employed. Plants producing PPI-I_CP933 fusion protein did not exhibit the severe toxic effects on apical shoot growth observed with cytoplasmic expression of CP933, indicating successful protein targeting. Since one of the aims of this work was to obtain functionally active CP933 protein, the fusion of CP933 (20.7 kDa) with GFP (26.3 kDa) for monitoring of CP933 localization in plant cells was avoided as this protein fusion could affect protein folding and consequently the activity of CP933.

Low protein expression in *N. benthamiana* may be due to the toxicity of CP933 itself, even after the vacuole targeting strategy was applied. Electrophoretic analysis revealed the difference in sizes between CP933 extracted with 1× PBS and 8 M urea buffer, where the protein migrated with the size of a dimer after treatment with 8 M urea. It has been reported that the Norovirus capsid P protein spontaneously formed dimers that were very stable over a broad range of pH (2 to 11) or under strong denaturing conditions (60 min of 8 M urea or 6 M guanidine treatment) [38]. Moreover, dimerization through the cysteine SH group of calreticulin (ubiquitous protein, located primarily in the endoplasmic reticulum) was induced by lowering the pH to 5–6, by heating, or in the presence of urea at a concentration above 2.6 M or an SDS concentration above 0.025% [18]. The same protein formed very stable oligomers through non-covalent interactions at concentrations of urea above 2.6 M (pH below 4.6 or above 10) at temperature above 40°C, or in the presence of organic solvents at high concentrations (25%) [18]. It may be that extraction of CP933 under denaturing conditions (using 8 M urea buffer) allows monomers to closely interact with each other, forming very stable dimers.

The antimicrobial activity of purified plant-produced PPI-I_CP933 protein, when added exogenously to the bacteria, was evaluated against *C. michiganensis* and *E. coli* BL21(DE3). *C. michiganensis* was more susceptible to CP933 treatment than *E. coli*. Current literature indicates that lysins, when added externally, preferably work against gram-positive bacteria, because of the ability of lysins to contact peptidoglycan of the cell wall directly, whereas the presence of the outer membrane in gram-negative bacteria makes lysin-peptidiglycan interaction difficult [13].

Our study showed that targeting of CP933 to the delta vacuoles using the signal peptide of the PPI-I protein protected plants against the toxic effect of the CP933 endolysin and allowed recovery of protein possessing antimicrobial activity. Thus, the combination of transient expression and protein targeting is a promising approach for the production of functionally active proteins that exhibit toxicity when expressed in *E. coli* and cytoplasmically in plant cells.

Acknowledgments

We thank Chris Pooley, Information Technology Specialist USDA, ARS, Electron and Confocal Microscopy Unit, Beltsville MD, USA for helping with design the of confocal laser scanning microscopy images. We acknowledge Dr. I.-M. Lee (Molecular Plant Pathology Laboratory, USDA, Beltsville MD, USA) for the gift of the *Clavibacter* phytopathogenic bacterial strain. Mention of trade names or commercial products in this publication is solely for the purpose of providing specific information and does not imply recommendation or endorsement by the USDA; USDA is an equal opportunity provider and employer.

References

1. Borisjuk NV, Borisjuk LG, Logendra S, Petersen F, Gleba Y, Raskin I. 1999. Production of recombinant proteins in plant root exudates. *Nat. Biotechnol*. **17:** 466-469.
2. Borysowski J, Weber-Dabrowska B, Gorski A. 2006. Bacteriophage endolysins as a novel class of antibacterial agent. *Exp. Biol. Med.* **231:** 366-377.
3. Chapman S, Kavanagh T, Baulcombe D. 1992. *Potato virus X* as a vector for gene expression in plants. *Plant J.* **2:** 549-557.
4. Company N, Nadal A, La Paz J-L, Martínez S, Rasche S, Schillberg S, *et al*. 2014. The production of recombinant cationic α-helical antimicrobial peptides in plant cells induces the formation of protein bodies derived from the endoplasmic

reticulum. *Plant Biotechnol. J.* **12:** 81-92.
5. Daniell H, Lee SB, Panchal T, Wiebe PO. 2001. Expression of the native cholera B toxin subunit gene and assembly as functional oligomers in transgenic tobacco chloroplasts. *J. Mol. Biol.* **311:** 1001-1009.
6. Donini M, Lico C, Baschieri S, Conti S, Magliani W, Polonelli L, Benvenuto E. 2005. Production of an engineered killer peptide in *Nicotiana benthamiana* by using a *Potato virus X* expression system. *Appl. Environ. Microbiol.* **71:** 6360-6367.
7. Donovan DM. 2007. Bacteriophage and peptidoglycan degrading enzymes with antimicrobial applications. *Recent Pat. Biotechnol.* **1:** 1-10.
8. Donovan DM, Becker SC, Dong S, Baker JR, Foster-Frey JA, Pritchard DG. 2009. Peptidoglycan hydrolase enzyme fusions are uniquely suited for treating multi-drug resistant pathogens. *Biotech. Int.* **21:** 6-10.
9. Drake PM, Chargelegue DM, Vine ND, van Dolleweerd CJ, Obregon P, Ma JK. 2003. Rhizosecretion of a monoclonal antibody protein complex from transgenic tobacco roots. *Plant Mol. Biol.* **52:** 233-241.
10. Düring K, Porsch P, Mahn A, Brinkmann O, Gieffers W. 1999. The non-enzymatic microbicidal activity of lysozymes. *FEBS Lett.* **449:** 93-100.
11. Filice GA, Nyman JA, Lexau C. 2010. Excess costs and utilization associated with *Staphylococcus aureus* infection. *Infect. Control Hosp. Epidemiol.* **31:** 365-367.
12. Fischetti VA. 2008. Bacteriophage lysins as effective antibacterials. *Curr. Opin. Microbiol.* **11:** 393-400.
13. Fischetti VA. 2010. Bacteriophage endolysins: a novel anti-infective to control gram-positive pathogens. *Int. J. Med. Microbiol.* **300:** 357-362.
14. Haddix AC, Teutsch SM, Corso PS. 2003. *Prevention Effectiveness: A Guide to Decision Analysis and Economic Evaluation*, pp. 345-357. 2nd Ed. Oxford University Press, New York.
15. Jackson MA, Nutt KA, Hassall R, Rae AL. 2010. Comparative efficiency of subcellular targeting signals for expression of a toxic protein in sugarcane. *Funct. Plant Biol.* **37:** 785-793.
16. Jauh G-Y, Fischer AM, Grimes HD, Ryan CA, Rogers JC. 1998. δ-Tonoplast intrinsic protein defines unique plant vacuole functions. *Proc. Natl. Acad. Sci. USA* **95:** 12995-12999.
17. Jauh G-Y, Phillips TE, Rogers JC. 1999. Tonoplast intrinsic protein isoforms as markers for vacuolar functions. *Plant Cell* **11:** 1867-1882.
18. Jørgensen CS, Ryder LR, Steinø A, Højrup P, Hansen J, Beyer NH, *et al*. 2003. Dimerization and oligomerization of the chaperone calreticulin. *Eur. J. Biochem.* **270:** 4140-4148.
19. Komarnytsky S, Borisjuk NV, Borisjuk LG, Alam MZ, Raskin I. 2000. Production of recombinant proteins in tobacco guttation fluid. *Plant Physiol.* **124:** 927-933.
20. Kovalskaya N, Hammond RW. 2009. Expression and functional characterization of the plant antimicrobial snakin-1 and defensin recombinant proteins. *Protein Expr. Purif.* **63:** 12-17.
21. Kovalskaya N, Zhao Y, Hammond RW. 2011. Antibacterial and antifungal activity of a snakin-defensin hybrid protein expressed in tobacco and potato plants. *Open Plant Sci. J.* **5:** 29-42.
22. Lacomme C, Chapman S. 2008. Use of *Potato virus X* (PVX)-based vectors for gene expression and virus-induced gene silencing (VIGS). *Curr. Protoc. Microbiol.* **8:** 16I.1.1-16I.1.13.
23. Lico C, Chen Q, Santi L. 2008. Viral vectors for production of recombinant proteins in plants. *J. Cell. Physiol.* **216:** 366-377.
24. Loeffler JM, Fischetti VA. 2003. Synergistic lethal effect of a combination of phage lytic enzymes with different activities on penicillin-sensitive and -resistant *Streptococcus pneumoniae* strains. *Antimicrob. Agents Chemother.* **47:** 375-377.
25. Loeffler JM, Nelson D, Fischetti VA. 2001. Rapid killing of *Streptococcus pneumoniae* with a bacteriophage cell wall hydrolase. *Science* **294:** 2170-2172.
26. Murray C, Sutherland PW, Phung MM, Lester MT, Marshall RK, Christeller JT. 2002. Expression of biotin-binding proteins, avidin and streptavidin, in plant tissues using plant vacuolar targeting sequences. *Transgenic Res.* **11:** 199-214.
27. Oliveira H, Melo LDR, Santos SB, Nóbrega FL, Ferreira EC, Cerca N, *et al*. 2013. Molecular aspects and comparative genomics of bacteriophage endolysins. *J. Virol.* **87:** 4558-4570.
28. Orito Y, Morita M, Hori K, Unno H, Tanji Y. 2004. *Bacillus amyloliquefaciens* phage endolysin can enhance permeability of *Pseudomonas aeruginosa* outer membrane and induce cell lysis. *Appl. Microbiol. Biotechnol.* **65:** 105-109.
29. Pang T, Fleming TC, Pogliano K, Young R. 2013. Visualization of pinholin lesions in vivo. *Proc. Natl. Acad. Sci. USA* **110:** E2054-E2063.
30. Pang T, Savva CG, Fleming KG, Struck DK, Young R. 2009. Structure of the lethal phage pinhole. *Proc. Natl. Acad. Sci. USA* **106:** 18966-18971.
31. Park T, Struck DK, Dankenbring CA, Young R. 2007. The pinholin of lambdoid phage 21: control of lysis by membrane depolarization. *J. Bacteriol.* **189:** 9135-9139.
32. Perna NT, Plunkett GIII, Burland V, Mau B, Glasner JD, Rose DJ, *et al*. 2001. Genome sequence of enterohaemorrhagic *Escherichia coli* O157:H7. *Nature* **409:** 529-533.
33. Rashel M, Uchiyama J, Ujihara T, Uehara Y, Kuramoto S, Sugihara S, *et al*. 2007. Efficient elimination of multidrug-resistant *Staphylococcus aureus* by cloned lysin derived from bacteriophage phi MR11. *J. Infect. Dis.* **196:** 1237-1247.
34. Saitoh H, Kiba A, Nishihara M, Yamamura S, Suzuki K, Terauchi R. 2001. Production of antimicrobial defensin in *Nicotiana benthamiana* with a *Potato virus X* vector. *Mol. Plant Microbe Interact.* **14:** 111-115.
35. São-José C, Parreira R, Vieira G, Santos MA. 2000. The N-terminal region of the *Oenococcus oeni* bacteriophage fOg44 lysin behaves as a bona fide signal peptide in *Escherichia coli* and as a *cis*-inhibitory element, preventing lytic activity on

oenococcal cells. *J. Bacteriol.* **182:** 5823-5831.
36. Schmelcher M, Donovan DM, Loessner MJ. 2012. Bacteriophage endolysins as novel antimicrobials. *Future Microbiol.* **7:** 1147-1171.
37. Shen Y, Mitchell MS, Donovan DM, Nelson DC. 2012. Phage-based enzybiotics, pp. 217-239. *In* Hyman P, Abedon ST (eds.). *Bacteriophages in Health and Disease.* CAB International, Wallingford, UK.
38. Tan M, Hegde RS, Jiang X. 2004. The P domain of novovirus capsid protein forms dimer and binds to histo-blood group antigen receptors. *J. Virol.* **78:** 6233-6242.
39. Tregoning JS, Nixon P, Kuroda H, Svab Z, Clare S, Bowe F, *et al*. 2003. Expression of tetanus toxin fragment C in tobacco chloroplasts. *Nucleic Acids Res.* **31:** 1174-1179.
40. Wang I-N, Deaton J, Young R. 2003. Sizing the holin lesion with an endolysin-beta-galactosidase fusion. *J. Bacteriol.* **185:** 779-787.
41. Wang I-N, Smith DL, Young R. 2000. Holins: the protein clocks of bacteriophage infections. *Annu. Rev. Microbiol.* **54:** 799-825.
42. Xu M, Struck DK, Deaton J, Wang I-N, Young RY. 2004. A signal-arrest release sequence mediates export and control of the phage P1 endolysin. *Proc. Natl. Acad. Sci. USA* **101:** 6415-6420.